Forensic Science International 318 (2021) 110601

Contents lists available at ScienceDirect

Forensic Science International

journal homepage: www.elsevier.com/locate/forsciint

The effects of camera resolution and distance on suspect height analysis using PhotoModeler

Angela M. Olver[a,*], Helen Guryn[b], Eugene Liscio[b]

[a] University of Toronto Mississauga, 3359 Mississauga Road, Mississauga, ON, L5L 1C6, Canada
[b] ai2-3D Forensics, 271 Jevlan Drive, Unit 14, Vaughan, ON, L4L 8A4, Canada

ARTICLE INFO

Article history:
Received 16 June 2020
Received in revised form 1 October 2020
Accepted 12 November 2020
Available online 18 November 2020

Keywords:
Forensic science
Suspect height analysis
Height estimations
Photogrammetry
PhotoModeler
3D laser scanning

ABSTRACT

The purpose of this study was to examine how camera resolution and suspect-camera distance affect the accuracy and precision of suspect height estimations using PhotoModeler software. Sixteen individuals were measured and recorded standing at 15 pre-set distances on 7 security cameras, each with a different resolution setting. A height scale was used to measure each individual's height prior to recording and was also used as a reference height. Height estimates were taken in PhotoModeler by extracting video frames that were calibrated using 3D point model data obtained from a laser scan of the test site. Errors were calculated for the measurements and compared using the Kruskal-Wallis H-test, which indicated significant differences for errors among different resolutions and distances ($p < 0.01$). Interaction plots, however, demonstrated little difference in errors for most resolutions and positions. The accuracy and precision of height estimates began to decrease with resolutions under 960H and distances over 36.5 m.

1. Introduction

Suspect height analysis involves the measurement of suspects caught on camera (e.g. surveillance video as a form of evidence [1,2]. It can allow investigators to eliminate potential suspects based on height differences from an individual caught on surveillance, or differentiate between multiple suspects recorded at a scene [3]. Methods used to estimate height include projective geometry (which utilizes vanishing points of parallel lines in a scene), 3D scene modelling, and photogrammetry [2,3]. Photogrammetry is the discipline of applying scientific methods to taking 3D measurements on photographs, and has been used for forensic purposes, such as suspect height analysis, for decades [4–6]. Photogrammetry involves the integration of physics and mathematics with technology to carry out measurements [4–6]. The reverse projection method involves the replication of the original camera (e.g. position, angles, field of view) and Digital Video Recorder (DVR) parameters present in the security system at a crime scene in order to capture new footage for measurement-taking that can be laid over footage of a suspect [4,7]. With the resulting images from the reverse projection method, an analyst can make overlays in image editing programs to take direct measurements on the photos. Photogrammetry using 3D data does not require one to return to the scene's original security system parameters, as the 3D data is used to digitally solve for the original camera parameters (i.e. camera resection) and calibrate the scene images in order extract accurate measurements [7]. As such, there are currently many novel techniques available to use with photogrammetry, including specialized software and laser scanners [5,6,8,9]. One such software is PhotoModeler, which is a comprehensive photogrammetry package that allows users to establish a camera's position and orientation and solve for camera parameters using 3D measurements [10]. Such 3D measurement data can be obtained via hand measuring (which, although easy to employ, can be inefficient and imprecise), total stations, and laser scanners, which employ the use of light to measure surroundings and collect points with a high degree of accuracy for the creation of scene models [8,9]. Laser scanning technology is the basis for LiDAR mapping, speed detection guns used by police agencies, robotic object classification, and many other devices and techniques.

PhotoModeler is a commonly used computer program in North America for estimating suspect height with photogrammetry, allowing users to take 3D measurements from digital photos and exported video still frames [2,5,10,11]. It can also calculate the source camera's position from a single photo or a still frame [10]. When measuring suspect height from an image, the pixels in the image are matched (i.e. referenced) to the corresponding 3D points such as those obtained from a laser scan point cloud of the scene

* Corresponding author at: Tel. +1 647 308 7322.
E-mail addresses: angela.olver@mail.utoronto.ca (A.M. Olver), helen@ai2-3d.com (H. Guryn), eliscio@ai2-3d.com (E. Liscio).

http://dx.doi.org/10.1016/j.forsciint.2020.110601
0379-0738/

[1,12]. Once enough points have been referenced, the camera's position, orientation and other parameters are calculated. A point on the ground is chosen as a "reference ground point", which is an estimate of where the vertex of the head is projected as a plumb line to the ground, where this plumb line intersects with the ground plane [1,12]. The point is then offset directly up on the Z-axis, which establishes the height measurement of the suspect [1,12].

A number of studies have validated the photogrammetry method for suspect height analysis, but there are four proposed categories of variables that can affect its application and outcomes [1,2,6,11,13,14]. Environmental effects involve the scene and include the number of features/objects present that can be used for referencing, and take into consideration things such as visibility, lighting, ground flatness and ground level [1,2,11,13,14]. Individual effects are suspect-specific, and include their posture, motion/gait, footwear, hair, headwear, and spinal compression or height variation throughout the day (approximately 1–3 cm change) [8,11,15]. Analyst effects can involve the technique used, where points are picked on a suspect to begin and end a height measurement, the number of references used to calibrate the images, and their quality. Camera effects include parameters such as the angle at which cameras are directed, their elevation, lens distortion, resolution settings and the distance between suspects and the camera [1,2,11,13,14]. Camera resolution has been found to affect the creation of 3D photogrammetric models in that models composed of higher resolution images are of higher quality and accuracy, with lower resolutions minimizing quality and accuracy; these findings apply only to the modelling aspect of photogrammetry and not its use for taking measurements [16].

The purpose of this research was to examine if camera resolution and suspect-camera distance affect the accuracy and precision of suspect height measurement using PhotoModeler. Currently there is a lack of research on how these two variables may impact the analysis of suspect height when this method is used. It is imperative that the accuracy and precision be known for investigative techniques that yield exclusionary evidence such as suspect height. Thus, the objective of this study is to provide a reference for analysts by assessing the effects of resolution and distance via standard errors and the reproducibility of measurements.

2. Materials and methods

Data collection was conducted in a parking garage at the University of Toronto Mississauga campus. The sample consisted of sixteen volunteer 'suspects' (men and women, 20–50 years, 150–180 cm tall). A stadia rod/height scale was used as a control height reference for the volunteers, and a FARO Focus S350 laser scanner (FARO, Lake Mary, FL) was used to take 10 scans using a scan resolution of 1/5 and quality setting of 3X. A 1/5 resolution setting amounts to a point spacing of 7.67 mm at 10 m, while the 3X quality setting was chosen for its use as a typical setting for crime scene documentation [17]. Black-and-white checkerboard targets were set up around the parking garage within the camera frames, so that they could be recognized by the laser scanner. The targets were also used as references for 3D model creation and subsequently used as reference points when solving for the cameras' positions using PhotoModeler later on. Seven Lorex security cameras, and a Lorex DVR (Lorex Technology Inc., Markham, ON, Canada) were used to record footage of the volunteers. The cameras were mounted to a wooden rig (constructed from wooden planks and a flat board) at an elevation of approximately 2.5 m, and all angled approximately 40 degrees downward to capture all distance markers within their field of view. The camera resolutions settings used are presented in Table 1. The distances were marked on the floor in a pathway using black duct tape and a metre measuring tape, shown in Fig. 1 and Table 2. The first distance marker was placed so that it was a close to the camera rig as possible while still within all fields of view. Distances #1–4 were placed 1 m apart, distances #4–7 were placed approximately 2 m apart, and all following distance markers were placed 5 m apart, to capture a wide range. The reference height scale was a hand-painted wooden board, calibrated using a measuring tape, and fitted with a level and sliding bar so that it could be used to measure the volunteers' heights prior to recording. Fig. 2 depicts the experimental setup.

The process was first performed by one of the researchers holding the height scale at each of the distance points on the path, as a controlled height artifact (i.e. human variation eliminated), before moving onto the volunteer suspects. The control measurement for the height scale was 200 cm (see Fig. 3). To measure the number of pixels that the height scale was composed of at every distance on every resolution setting, the still images of the height scale were imported into Adobe Photoshop (Adobe Inc., San Jose, CA), the units in the program were set to pixels, and the ruler tool was used to measure the height scale from its base to the 200 cm mark. The pixel measurements of the height scale at every resolution setting and distance point were then put into ratios of cm/pixel. This ratio is helpful as it provides an estimate of the error that will occur for every pixel that an analyst is off when measuring height on a still image, at a given resolution and distance. After a suspect's height was measured with a stadia rod (i.e. ground truth height measurement), they were instructed to stand at the first distance marker on the pathway with their back facing the camera. After one distance point along the pathway was captured (i.e. a sufficient image retained, observed from the camera feed on the monitor), they moved to the next marked distance point, and this was repeated until the person had been captured standing at all marked distances along the ground pathway. This process was repeated with all the volunteer suspects.

The programs used in this research include iNPUT-ACE (iNPUT-ACE, Spokane, WA), FARO SCENE, Autodesk 3 ds Max (Autodesk Inc., San Rafael, CA), and PhotoModeler Premium (Eos Systems Inc., Vancouver, BC, Canada). iNPUT-ACE was used to extract the still frames from the video footage as. bmp files of the scene and the suspects standing along the pathway for the creation of the photogrammetry models. FARO SCENE was used to process and register the laser scans together to create a 3D point cloud model of scene. Subsequently, the point cloud data was imported into Autodesk 3 ds Max, a modelling software in which the 3D scene was reduced to a collection of points outlining the main features of the scene and the location of the centres of the checkerboard targets. Planes were created on the 'floor' of the 3D scene model where the distance markers were located to facilitate height

Table 1
Resolution settings assigned to each camera.

Camera No.	1	2	3	4	5	6	7
Assigned Resolution	4 K (3840 × 2160)	1440p (2560 × 1440)	1080p (1920 × 1080)	720p (1280 × 720)	960H (960 × 480)	480p (704 × 480)	240p (352 × 240)

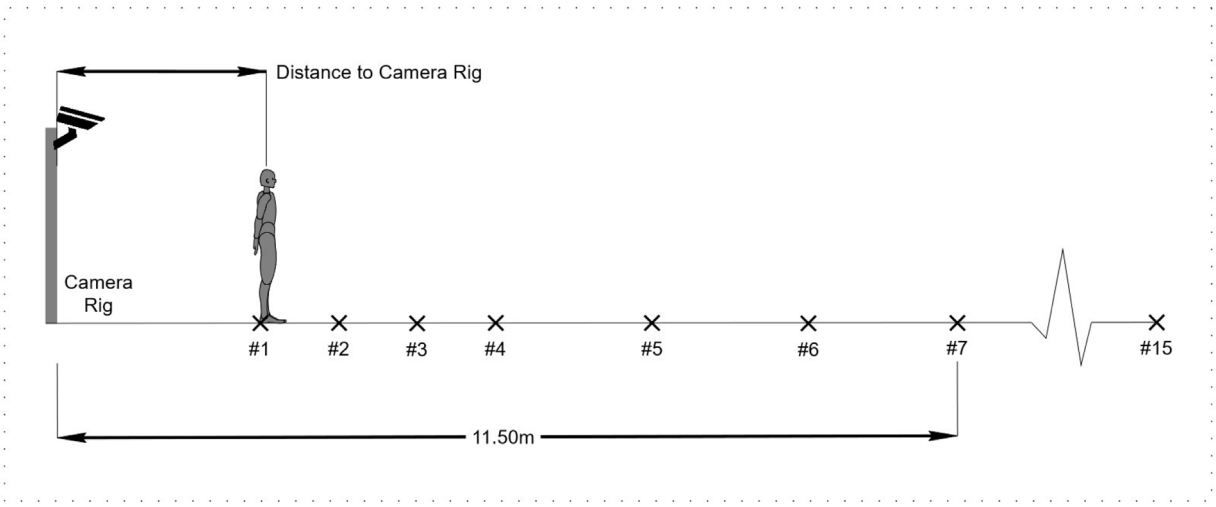

Fig. 1. Side-view of experimental setup with placement of distance markers on the ground.

Table 2
Distances marked on the ground in metres.

Marker No.	1	2	3	4	5	6	7	8	9	10	11	12	13	14	15
Distance	2.6 m	3.6 m	4.6 m	5.6 m	7.6 m	9.6 m	11.5 m	16.5 m	21.5 m	26.5 m	31.5 m	36.5 m	41.5 m	46.5 m	51.5 m

Fig. 2. Experimental setup, featuring a FARO Focus S350 terrestrial laser scanner, Lorex camera rig, DVR and monitor.

measurements in PhotoModeler. The concrete floor in the parking garage was uneven, so separate smaller planes had to be created at each distance marker to facilitate the analysis and eliminate a potential external source of error. The subsampled 3D model (composed of points and lines in the. DXF format) was imported into PhotoModeler, along with the empty reference frames. A separate project file was created in the program for each camera. With the empty reference frame for a camera loaded, points in the 3D model (the centre of the targets, corners of objects in the scenes, etc.) were matched to their corresponding pixel location in the reference frame to calibrate it (see Fig. 4). The floor planes were then imported onto the still image. Separate photogrammetry models were created for each suspect standing at all 15 distance points for each camera, using the corresponding calibrated reference frame as the first image in each image sequence.

To measure each suspect's height on the extracted frames, a point was chosen at the suspect's feet and a Z-axis offset was created to make a straight line from the feet to the vertex of the head. Depending on the proximity of the suspect to the cameras, the bottom point was either chosen between and in the centre of the suspect's feet (for closer distances, as the cameras had a more downward-looking perspective on the suspects) or at their heels (for farther distances, where suspects appeared perpendicular to the cameras). The line was adjusted until the endpoint properly met the top of the head. The length of the straight line, equivalent to the height measurement, was recorded in the data table for that suspect at that distance point for the chosen camera. This process was then repeated for all distances, suspects and cameras (see Fig. 5).

A total of 1446 height estimates (data entries) were taken. Errors and absolute errors for the entire data set were calculated based on the differences between the actual/measured suspect heights and height estimates, and then sorted by camera and distance. Standard deviations were calculated from the height estimates for each resolution setting and distance point by suspect, then averaged. Height estimates could not be completed for distances #7–15 with the 480p and 240p cameras, as the placement of the timestamp in the frames obstructed the view of the farthest distances and hence the suspects' heads. As such, there were fewer data points for cameras #6 and #7. Statistical tests were performed using Minitab (Minitab, LLC; State College, PA), RStudio (RStudio, PBC; Boston, MA), and Microsoft Excel (Microsoft, Redmond, WA). Probability distributions were calculated using the Kolmogorov-Smirnov test for normality. The KS-

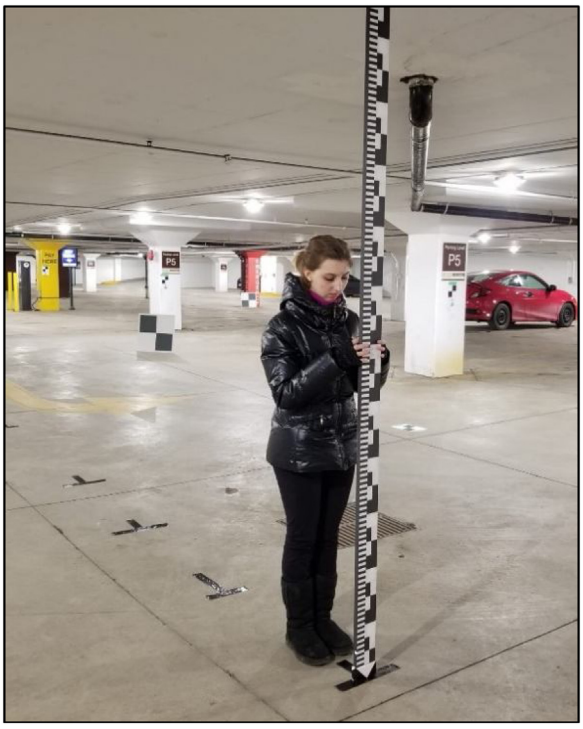

Fig. 3. Researcher conducting first trial using the height scale as a reference/control, standing at the first distance marker.

test assesses whether a set of data follows a normal distribution pattern, in which the data would resemble a 'bell curve' [18]. The Kruskal-Wallis H-test was performed on the errors for camera resolution and distance separately, to evaluate the effects of each on accuracy (criteria of $p < 0.05$ used, α=95%). The Kruskal-Wallis H-test is a non-parametric test (i.e. can be performed on data that is not normally distributed) used to determine whether there are statistically significant differences between groups of data according to associated variables (e.g. resolution and distance) [19]. A *post hoc* Dunn test was performed to compare the errors; this statistical test is used to compare groups of non-parametric data as a cross-check for Kruskal-Wallis test results to determine how the groups differ [20].

3. Results

3.1. Accuracy with measurement errors

The errors between known participant heights and all height estimate data, including outliers, ranged from a -4.0 cm underestimation of height to a 4.7 cm overestimation, with approximately 75% of the errors (including absolute and relative) falling below +/- 1.3 cm (see Fig. 6). The absolute error range was between 0.0–4.7 cm. Four outliers were pinpointed amongst the data, and when removed, the maximum measurement error (for both absolute and relative errors) was an overestimation 3.4 cm, on camera #7 (240p) at distance #1 (2.6 m). The four outliers were errors of 3.8 cm on camera #3 (1080p) at distance #12 (36.5 m), 3.8 cm on camera #7 at distance #1, -4.0 cm on camera #5 (960 H) at distance #14 (46.5 m), and 4.7 cm on camera #5 at distance #12. The Kolmogorov-Smirnov test performed on the height estimate data showed that the errors and absolute errors were not normally distributed ($p < 0.010$). Tables 3 and 4 provide the average absolute measurement errors by suspect, for camera resolution and for distance, respectively. Table 5 provides the average absolute errors of the height estimates at a given resolution setting and distance position (e.g. at a resolution of 4 K at a distance of 2.6 m, an average error of 1.318 cm was recorded).

As the data was not normally distributed, a non-parametric statistical test was employed. The results of the two Kruskal-Wallis H-tests, one for the resolution variable and one for the distance variable, were a *P*-value of < 0.01 for both, indicating a significant difference in the medians of the errors for the distances and resolution settings (criteria of $p < 0.05$ used, α=95%). The *post hoc* Dunn test demonstrated that distance points #1 (2.6 m), #10 (26.5 m), #11 (31.5 m), #12 (36.5 m), #13 (41.5 m), #14 (46.5 m) and #15 (51.5 m) were most comparable in terms of having significant differences from the median error ($p < 0.01$). The Dunn test also revealed that there were no significant differences between distance points #2–11; there were small differences indicated between cameras #2 (1440p), #4 (720p) and #6 (480p).

The Fig. 7 and 8 interaction plots demonstrate the median variation in errors by suspect-camera distance and camera resolution. The median errors by distance in Figs. 7 and 8 mostly fall beneath a value of 1.5 cm. The exceptions are distance points #1 (2.6 m) and #12 (36.5 m) in Fig. 7, and cameras #5 (960 H) and #7 (240p) in Fig. 8, which have higher median errors that peak at approximately 2.25–2.5 cm for both. Figs. 9 and 10 depict the errors solely for the height scale, by suspect-camera distance and camera

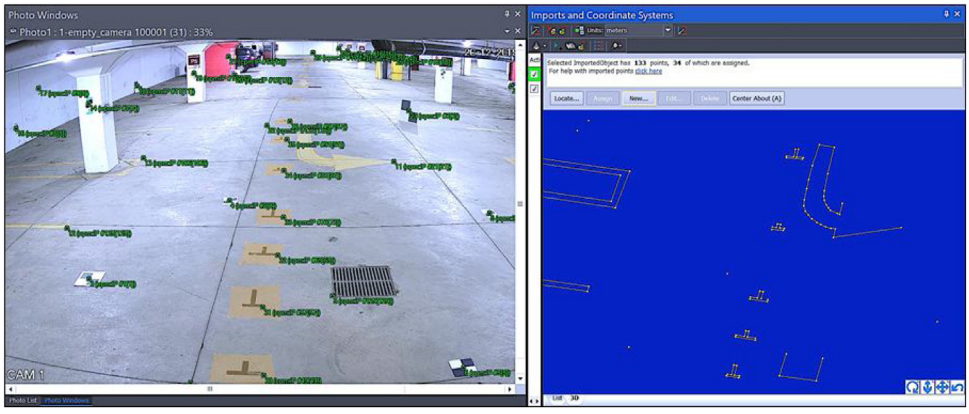

Fig. 4. PhotoModeler workspace, with reference frame of the scene [left] and a subsample of 3D points [right] loaded for the referencing process. Pathway of distance markers down centre.

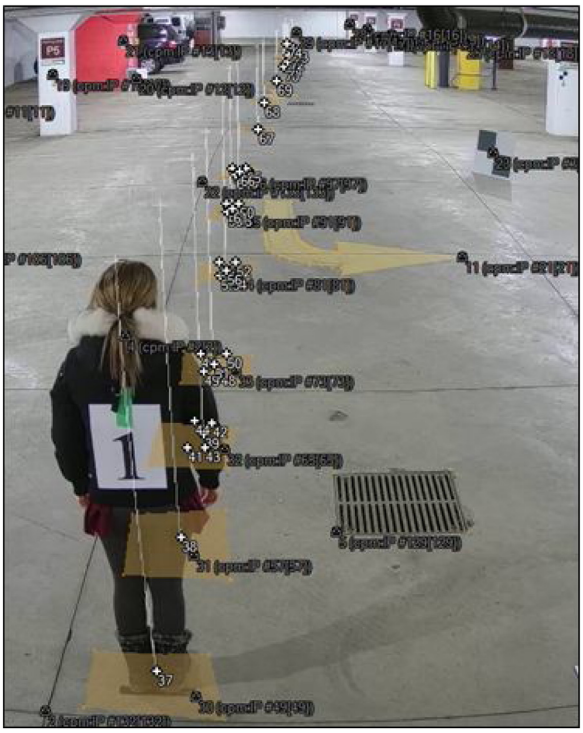

Fig. 5. PhotoModeler workspace, depicting 'suspect #1' standing along the pathway at distance marker #1 on the first camera [4 K resolution], with all height estimates taken.

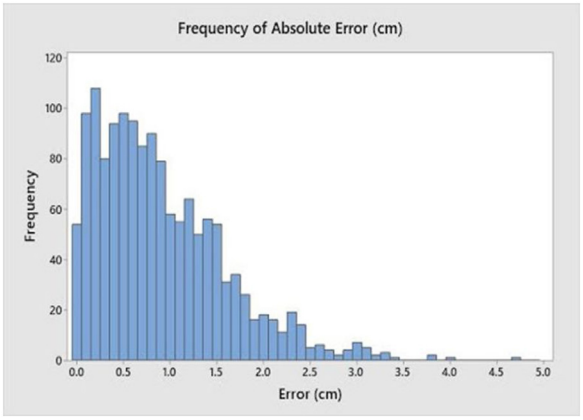

Fig. 6. Histogram of error (cm) frequency distributions [i.e. what amounts of errors are most common]. With the exception of four outliers, all other errors fall below 3.5 cm.

resolution, respectively. Estimates could not be taken for some of the distances and resolution settings with the height scale due to changes in ceiling height and overhanging pipes, which obstructed the 200 cm mark on the height scale at certain positions with certain fields of camera view and hence prevented reliable measurements. The control height was approximately 20 cm taller than the tallest 'suspect', so these obstructions were not an issue for taking other measurements.

3.2. Precision

The standard deviations of the height estimates from the means, by camera resolution and by suspect-camera distance, were calculated in Excel and ranged +/- 0.45–1.17 cm on average (see Tables 6 and 7). The first distance point (2.6 m) was noted to have a mean standard deviation of +/- 0.65 cm, while the average standard deviations for distances #2–9 ranged +/- 0.45–0.57 cm and began to exceed +/- 0.65 cm again with distance point #10 and farther. Camera #5 (960 H) and distance point # 14 (46.5 m) had the highest average standard deviations at approximately +/- 1.0 cm and +/- 1.17 cm, respectively. Distance #14 also had the highest overall standard deviation value that was recorded, at +/- 2.28 cm.

3.3. Accuracy in marking the height scale

The height scale (Fig. 3) served as a control subject with a reference height of 200 cm in this study. To determine the accuracy of measuring the height scale at different camera resolutions and distances, the number of pixels formed by the height scale in the various still frames (at all resolutions settings and at all assessed distance points) were quantified and put into a centimetre-per-pixel ratio (i.e. 200 cm height divided by the pixel measurement of the height scale in a given still frame), expressed in Table 8.

4. Discussion

4.1. Accuracy

There were discrepancies present between the *P*-values calculated and the distribution of the error data in the interaction plots. Though the notably low *P*-value of < 0.01 indicated a significant difference in the estimate errors, Figs. 7 and 8 showed few distinct trends. Despite the indication of minute differences for errors by camera resolution, Fig. 8 especially did not demonstrate any specific trend. There was some increase in error at cameras #5–7 for some of the distance positions, but this increase was not consistent. Fig. 7 for median errors by distance demonstrated that there was little to no variation in errors for distance points #2–11, as errors generally fell within the same range, with an increase only after distance #11 (31.5 m). Positions #1 and #12 had the highest error, which was inconsistent with the distances following position #1, and distances #13–15, which while increased from position #11, were not as notably high as the error at position #12. Regardless, the results suggested that the accuracy of suspect height estimates began to decrease at distances of 36.5 m and greater. Overall, this visual data suggested that the differences in the errors between the varying resolutions and distances were not as significant as the Kruskal-Wallis test results indicated. The Dunn test results reported a significant difference in errors between camera #2 (1440p) and camera #6 (480p). The difference reported between cameras #2 and #4 (720p), however, may be influenced by another untested factor. Distance position #4, 5.5 m, was found to have the lowest error of all seven camera resolutions, with median errors ranging 0.4–0.6 cm.

Three out of the four outliers were associated with distances of 36.5 m or farther (i.e. distance point #12). A higher error at distance #12 was more to be expected as it was farther along the pathway, but the median errors for distances #13-#15 ranged between 0.5–1.5 cm. This suggested that there may have been a confounding variable introduced at the two noted distance points, such suspects changing their posture, or standing with their heels just behind or in front of the back edge of the distance marker on the floor. The proximity of distance #1 to the security camera rig may have caused participants to be captured such that the camera-to-head angle made the vertices on the heads appear higher than in reality. This, in turn, would have affected pixel-picking when completing a height measurement. This would have led to an overestimation of height at this distance position, and hence higher error. Some

Table 3
Average absolute errors (cm) of the height estimates (compared to actual heights) by camera resolution.

Resolution Suspect	1–4 K	2–1440p	3–1080p	4–720p	5–960H	6–480p	7–240p
Height Scale Ref.	0.293	0.520	0.471	0.8	1.175	0.417	1.280
1	0.607	0.800	0.560	0.8933	0.980	0.920	1.650
2	0.707	1.540	1.553	0.96	1.327	1.380	1.583
3	0.647	1.120	0.907	1.1467	1.240	0.840	1.660
4	1.227	1.140	1.707	1.4667	1.187	1.060	1.080
5	0.807	0.427	0.740	0.8133	0.887	0.700	1.260
6	0.707	0.560	0.660	1.08	0.853	0.360	0.860
7	0.833	0.907	1.087	1.1267	0.907	1.140	1.140
8	0.680	0.653	1.027	0.8467	0.780	1.260	0.483
9	0.633	0.660	0.953	0.72	0.653	0.600	1.140
10	0.940	1.007	0.733	0.86	1.560	0.840	1.420
11	0.507	0.653	0.853	0.8733	0.979	0.580	1.250
12	0.813	0.847	0.693	0.7533	1.033	0.580	0.940
13	1.113	0.967	0.640	0.76	1.260	0.720	1.260
14	1.207	0.920	0.667	1.1933	0.880	0.720	1.020
15	0.473	0.400	1.233	1.1533	1.413	1.080	0.583
16	0.960	0.473	0.453	0.9	0.807	0.520	0.750
Average:	0.774	0.799	0.879	0.9616	1.054	0.807	1.139

Table 4
Average absolute errors (cm) of the height estimates by distance.

Distance Suspect	1–2.6 m	2–3.6 m	3–4.6 m	4–5.6 m	5–7.6 m	6–9.6 m	7–11.5 m	8–16.5 m	9–21.5 m	10–26.5 m	11–31.5 m	12–36.5 m	13–41.5 m	14–46.5 m	15–51.5 m
Height Scale Ref.	0.529	0.543	0.329	0.400	0.800	0.733	0.660	0.780	0.740	0.600	1.150	0.780	1.220	0.267	0.367
1	2.600	0.929	0.586	0.414	1.071	0.583	0.300	0.580	0.640	0.320	0.600	0.840	0.760	0.840	1.000
2	2.457	1.271	1.329	0.743	0.414	0.617	0.420	1.520	1.160	1.140	1.520	1.720	1.400	1.080	2.140
3	1.929	1.643	0.571	0.371	0.486	0.540	0.500	1.160	1.140	1.100	1.280	1.720	0.640	1.320	1.280
4	0.457	0.443	1.071	1.300	1.814	1.800	1.740	1.360	1.220	1.840	1.520	1.260	1.780	1.820	0.860
5	1.243	0.729	0.414	0.386	0.729	0.560	0.640	0.760	0.620	0.820	0.760	1.420	0.780	0.560	1.160
6	1.071	0.600	0.657	1.129	0.457	0.620	0.580	0.60	0.620	0.600	0.380	0.960	1.140	0.700	1.120
7	0.771	1.500	1.800	0.729	1.200	0.940	0.980	0.720	1.000	0.580	0.640	1.040	1.000	1.020	0.540
8	0.543	0.757	1.043	1.029	1.286	0.917	0.660	0.420	0.760	0.900	0.280	1.120	0.700	0.840	0.500
9	0.929	0.714	0. 600	0.629	0.829	0.720	0.800	0.560	0.380	0.400	0.560	0.980	0.960	1.560	0.500
10	2.457	0.971	0.614	0.457	0.343	0.720	0.540	0.960	0.840	0.540	1.060	2.580	1.120	1.220	1.200
11	2.186	0.429	0.400	0.314	0.629	0.283	0.640	0.600	0.050	1.060	0.780	1.340	0.660	1.100	0.920
12	1.671	0.471	0.314	0.257	0.871	0.260	0.480	0.460	0.680	0.800	1.300	1.400	0.920	1.260	1.360
13	1.157	0.671	0.600	0.843	0.471	0.540	0.520	1.020	0.920	0.880	1.080	2.320	1.260	1.120	1.300
14	1.871	0.857	0.529	0.371	0.386	0.480	0.780	1.100	0.940	0.860	0.840	1.540	1.180	1.380	1.620
15	1.100	0.486	0.929	0.843	1.257	1.133	1.280	0.600	0.280	0.720	0.720	0.340	1.260	1.700	1.080
16	1.671	0.729	0.443	0.257	0.314	0.300	0.420	0.660	0.580	0.520	0.760	1.740	0.380	1.100	0.900
Average:	1.449	0.808	0.719	0.616	0.786	0.691	0.702	0.815	0.766	0.805	0.896	1.588	1.009	1.111	1.049

Table 5
Average absolute errors (cm) of the height estimates by resolution and by distance.

Resolution Distance	1–4 K	2–1440p	3–1080p	4–720p	5–960H	6–480p *	7–240p *	*Average for Distance:*
1–2.6 m	1.318	1.453	0.959	1.429	1.412	1.340	2.241	1.450
2–3.6 m	0.671	0.712	0.671	0.712	0.912	0.780	1.206	0.808
3–4.6 m	0.676	0.635	0.765	0.7	0.694	0.680	0.882	0.719
4–5.6 m	0.594	0.635	0.659	0.694	0.518	0.490	0.724	0.616
5–7.6 m	0.718	0.618	0.953	1.029	0.700	0.730	0.753	0.786
6–9.6 m	0.671	0.665	0.629	0.818	0.635	0.800	0.733	0.707
7–11.5 m	0.647	0.518	0.776	0.882	0.688	–	–	0.702
8–16.5 m	0.782	0.665	0.735	0.924	0.971	–	–	0.815
9–21.5 m	0.735	0.659	0.712	0.753	0.971	–	–	0.766
10–26.5 m	0.741	0.582	0.859	0.876	0.965	–	–	0.805
11–31.5 m	0.929	0.871	0.618	0.806	1.188	–	–	0.882
12–36.5 m	0.765	0.800	1.682	1.294	2.253	–	–	1.359
13–41.5 m	0.676	0.959	1.118	0.941	1.353	–	–	1.009
14–46.5 m	0.871	1.041	1.076	1.459	1.076	–	–	1.105
15–51.5 m	0.812	1.182	0.941	1.059	1.212	–	–	1.041
Average for Camera Resolution:	0.774	0.800	0.877	0.958	1.036	0.800	1.090	

* Height estimates could not be completed for distances #7–15 with these cameras, as the placement of the timestamp in the frames obstructed the view of the farthest distances and hence the suspects' heads.

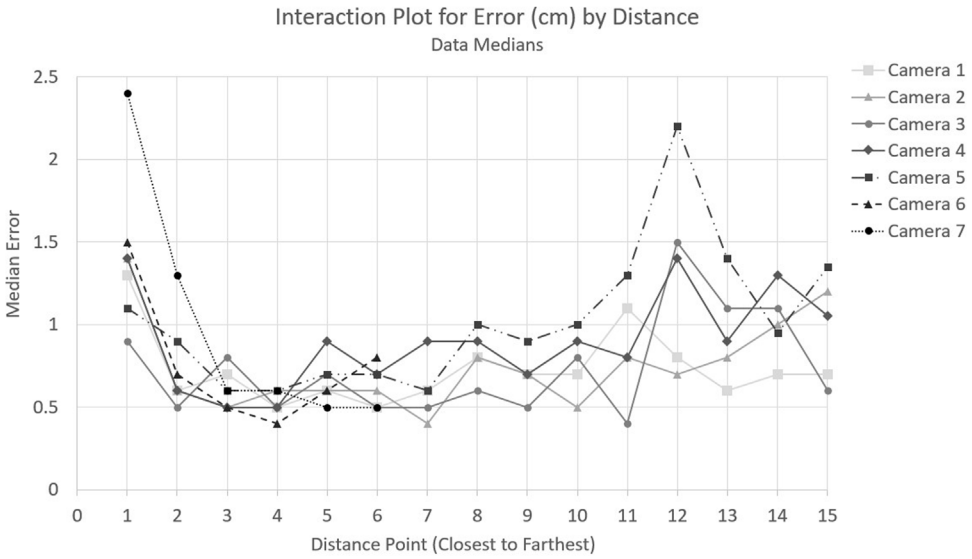

Fig. 7. Median errors (cm) by suspect-camera distance.

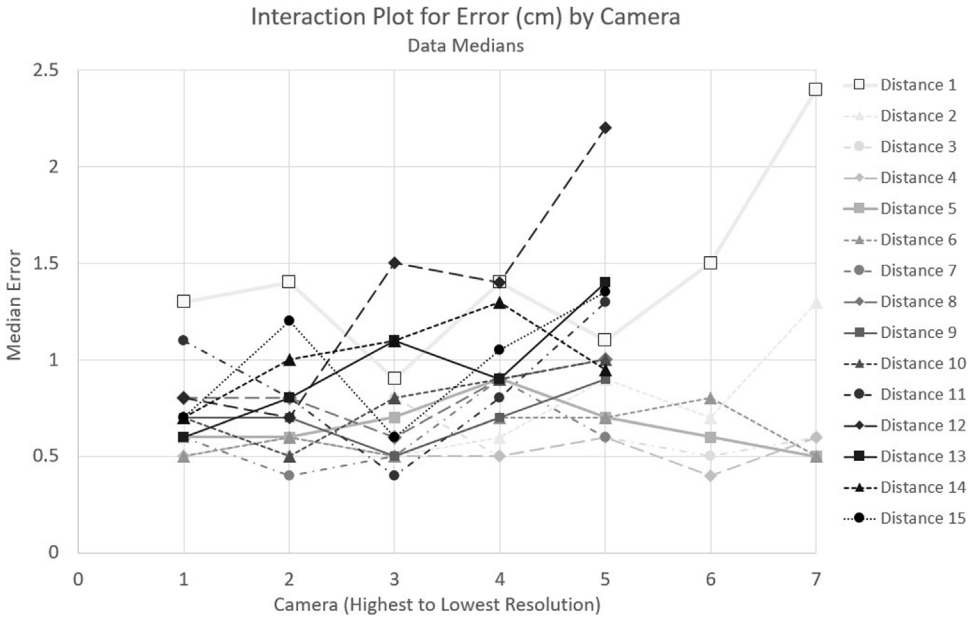

Fig. 8. Median errors (cm) by camera resolution.

camera angle distortion may have also been occurring at position #12 as well to cause the higher amount of error observed.

The four outliers present in the error data (above 3.5 cm) were removed from the data sets after the first round of statistics, due to the large sample size, so that the errors may be analyzed a second time. Again, the Kolmogorov-Smirnov tests for normality showed that the errors and absolute errors were not normally distributed, with little visual difference between the first and second probability plots, and the Kruskal-Wallis H-test again provided *P*-values of < 0.01 for resolution and distance. This number of outliers is relatively very small considering that there were over 1400 data entries analyzed.

Regarding the accuracy in marking the height scale (reference/control height of 200 cm), it can be observed in Table 8 that the centimetre-per-pixel ratios grew larger as distances increased and camera resolution decreased. This is due to the fact that the height scale is composed of fewer and fewer pixels in images that are of lower image quality, and/or that are taken of subjects that are further away. As such, measurement errors are greater (i.e. more significant) for every pixel underestimated or overestimated in a measurement on a still image. The centimetre-per-pixel ratios and the average absolute error for the height scale (see Table 4) were observed to be small at distance #1 (2.6 m), indicating that a more accurate height measurement can be taken at this distance. By contrast in this study, suspect height tended to be overestimated (i.e. higher errors), with the average absolute errors most often exceeding that of the height scale, at the first distance of 2.6 m. Since the reference height on the scale was 200 cm, about 20 cm higher than the tallest volunteer 'suspect', the camera-to-'head' angle from the security cameras to the reference height was smaller in comparison to what it would be for the 'suspects', minimizing the potential effect of this confounding variable on the accuracy outlined by the centimetre-per-pixel ratios that focus upon resolution and distance (Table 8). This further supports the

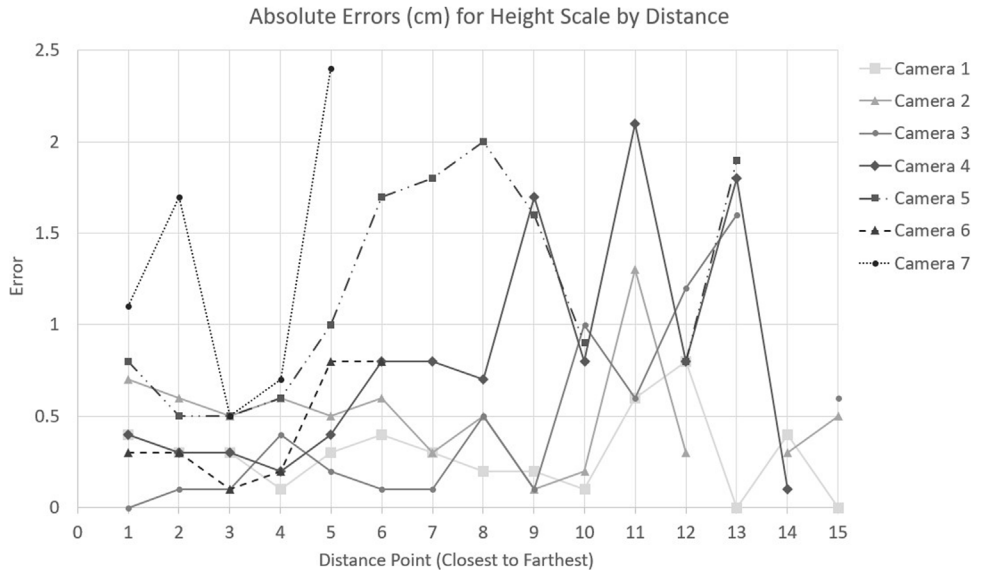

Fig. 9. Absolute errors (cm) for the control height scale only by suspect-camera distance.

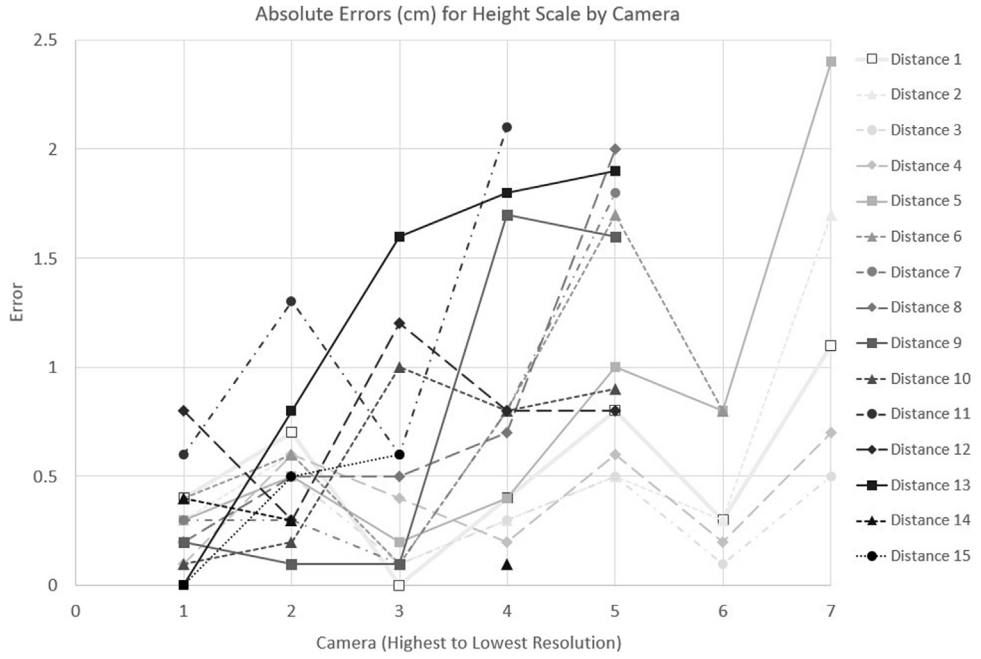

Fig. 10. Absolute errors (cm) for the control height scale only by camera resolution.

finding that height measurement accuracy of human subjects is affected by closer suspect-camera distances, such as by the occurrence of larger camera-to-head angles at these distances that distort the appearance of vertices on the head.

4.2. Precision

Based on the patterns observed with the standard deviation values, height estimates were most precise with higher resolution (i.e. standard deviations tended to be lower). The average standard deviations increased as camera resolution settings lowered, beginning at +/- 0.56 cm for camera #1 (4 K) and reaching +/-0.93 cm for camera #7 (240p). There was a steadier increase in standard deviations as camera resolution decreased, than can be observed with the errors (i.e. less fluctuation with precision than with accuracy). Interestingly, camera #5 (960 H) had the highest standard deviation of all resolution settings at +/- 1.01 cm, as opposed to one of the two lower resolution settings (480p or 240p). Slightly lower standard deviations at cameras #6 and #7 may have been influenced by the fact that fewer height estimates could be taken with these cameras, as previously discussed. Precision tended to decrease at farther distances, as standard deviations increased toward +/- 1 cm on average beginning at 26.5 m (distance #10) away and reaching above +/- 1 cm at 36.5 m away (distance #12). The exception was distance position #1 (2.6 m), which had a higher standard deviation (+/- 0.65 cm) than the following distances #2–9 which ranged from 3.6 to 21.5 m away, suggesting that another factor such as the camera-to-head angle can influence precision at close distances.

Table 6
Standard deviations of the height estimates (cm) by camera resolution.

Resolution Suspect	1–4 K	2–1440p	3–1080p	4–720p	5–960H	6–480p	7–240p
Height Scale Ref.	0.2336	0.3907	0.6318	0.6312	0.8107	0.3061	0.7759
1	0.9610	1.1288	0.7750	1.0909	1.0743	1.3472	0.9028
2	0.4301	0.6127	1.2803	1.0239	0.9280	0.8319	1.1496
3	0.4693	0.5240	0.6519	1.0618	0.7845	0.8019	0.9154
4	0.6703	0.7051	0.7948	0.7348	1.1155	0.9975	1.1059
5	0.6875	0.5397	1.0528	0.9460	0.8254	1.0173	0.8142
6	0.5668	0.6674	0.7894	1.0169	1.0288	0.4615	1.1082
7	0.5668	0.7370	0.7196	0.8417	1.0636	0.7861	1.3773
8	0.3877	0.7690	0.8268	0.8207	0.9884	0.5273	0.6969
9	0.4673	0.6829	0.6905	0.9270	0.7917	0.3742	0.7092
10	0.6092	0.7564	1.0157	0.9309	0.8624	0.8204	0.9524
11	0.4896	0.6638	1.0657	1.0264	1.3488	1.1059	1.3323
12	0.6638	0.7170	0.9184	0.9239	1.0736	0.9990	0.9529
13	0.4704	0.4701	0.8681	0.6651	1.1217	0.2775	0.3362
14	0.8102	0.5647	0.8779	1.4352	1.0450	1.0941	0.7759
15	0.5975	0.4998	0.7912	1.1716	1.2907	1.0977	0.8796
16	0.5369	0.4256	0.6139	1.2727	1.0163	0.7503	1.0759
Average:	0.5658	0.6385	0.8449	0.9718	1.01	0.7998	0.9330

Table 7
Standard deviations of the height estimates (cm) by suspect-camera distance.

Distance Suspect	1–2.6 m	2–3.6 m	3–4.6 m	4–5.6 m	5–7.6 m	6–9.6 m	7–11.5 m	8–16.5 m	9–21.5 m	10–26.5 m	11–31.5 m	12–36.5 m	13–41.5 m	14–46.5 m	15–51.5 m
Height Scale Ref.	0.364	0.535	0.180	0.385	0.824	0.543	0.733	0.710	0.875	0.581	0.714	0.847	0.808	0.153	0.551
1	0.408	0.582	0.565	0.519	0.671	1.011	0.462	0.383	0.676	0.422	0.785	0.907	0.901	1.012	1.478
2	0.989	0.594	0.411	0.432	0.267	0.387	0.385	0.618	0.808	0.723	1.031	1.544	0.943	1.333	0.730
3	0.615	0.565	0.583	0.398	0.573	0.594	0.476	0.207	0.167	0.400	0.259	1.035	0.439	0.835	0.683
4	0.321	0.351	0.364	0.332	0.402	0.636	0.532	0.647	0.370	0.297	0.545	1.065	0.630	1.377	0.764
5	1.041	0.588	0.546	0.580	0.660	0.502	0.849	0.981	0.880	0.950	0.996	1.370	1.055	0.730	0.498
6	1.405	0.361	0.562	0.655	0.390	0.295	0.404	0.661	0.731	0.381	0.492	0.808	1.014	0.915	1.299
7	0.678	0.277	0.238	0.535	0.424	0.623	0.409	0.483	0.292	0.701	0.661	1.294	1.057	1.221	0.673
8	0.679	0.506	0.404	0.519	0.430	0.708	0.649	0.539	0.378	0.596	0.327	1.242	0.888	1.099	0.744
9	0.683	0.748	0.653	0.758	0.918	0.782	0.826	0.752	0.228	0.444	0.760	1.085	1.195	1.689	0.579
10	0.387	0.320	0.324	0.519	0.257	0.476	0.594	0.385	0.770	0.795	0.577	0.867	1.246	0.497	0.667
11	0.827	0.482	0.501	0.382	0.817	0.355	0.796	0.158	0.212	1.295	0.756	1.210	0.730	1.262	1.032
12	0.446	0.398	0.316	0.344	0.427	0.370	0.536	0.336	0.438	0.784	0.700	0.381	0.939	1.441	1.161
13	0.525	0.439	0.365	0.493	0.516	0.451	0.385	0.259	0.657	0.507	0.409	1.583	0.844	0.876	0.752
14	0.658	1.017	0.624	0.367	0.515	0.422	0.581	0.453	0.416	0.726	0.541	0.948	1.410	1.879	1.123
15	0.469	0.479	0.531	0.717	0.716	0.596	0.460	0.800	0.192	0.886	1.043	0.367	1.046	2.280	1.208
16	0.594	0.479	0.540	0.340	0.382	0.455	0.534	0.592	0.691	0.785	0.498	1.262	0.439	1.217	1.089
Average:	0.652	0.513	0.453	0.487	0.541	0.542	0.565	0.527	0.517	0.663	0.653	1.048	0.917	1.166	0.884

Table 8
Centimetre-per-pixel ratios (cm) expressing the accuracy of measuring the control height scale at all resolutions and distances.

Resolution Distance	1–4 K	2–1440p	3–1080p	4–720p	5–960H	6–480p	7–240p
1–2.6 m	0.12	0.18	0.24	0.36	0.54	0.54	1.09
2–3.6 m	0.15	0.22	0.3	0.45	0.67	0.67	1.35
3–4.6 m	0.18	0.28	0.37	0.55	0.83	0.83	1.68
4–5.6	0.22	0.33	0.44	0.66	1	0.99	2
5–7.6 m	0.29	0.44	0.58	0.87	1.32	1.32	2.63
6–9.6 m	0.37	0.55	0.74	1.1	1.67	1.67	~ 3.77
7–11.5 m	0.44	0.66	0.89	1.32	2	–	–
8–16.5 m	0.64	0.95	1.27	1.9	2.86	–	–
9–21.5 m	0.83	1.24	1.67	2.5	3.77	–	–
10–26.5 m	1.03	1.54	2.04	3.08	4.65	–	–
11–31.5 m	~ 1.22*	~ 1.79	~ 2.38	~ 3.64	~ 5.56	–	–
12–36.5 m	1.43	2.13	2.86	4.26	6.45	–	–
13–41.5 m	1.63	2.41	3.28	4.76	7.41	–	–
14–46.5 m	1.83	2.74	4	5.71	8.7	–	–
15–51.5 m	2	2.99	4.17	6.45	10	–	–

* Ratios marked with "~" denotes an approximation; a scene feature at these distances (overhanging pipe, or the date/timestamp on camera #7 at distance #6) made measurement of the height scale more difficult to complete.

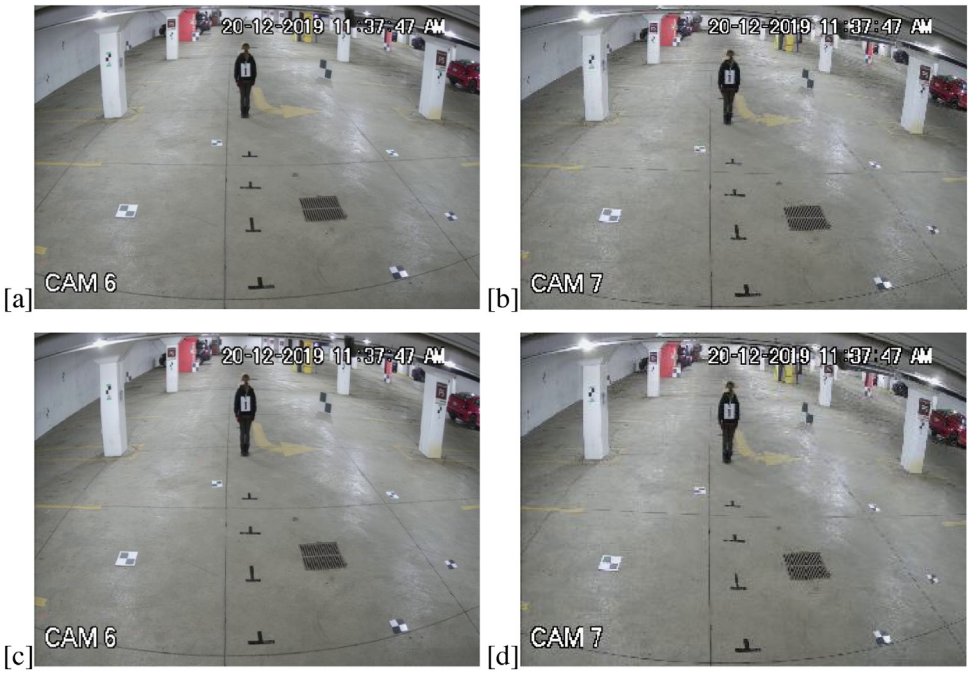

Fig. 11. Still frames from cameras [a,c] #6 (480p) and [b,d] #7 (240p) depicting how the timestamp would obstruct the suspects' heads at distances #7-15. Suspect is standing at distance #5 (7.6 m) with the timestamp already close above. Still frames in [a] and [b] are in the original computer-displayed aspect ratio of 1:1, while the still frames in [c] and [d] are in the corrected aspect ratio of 4:3 as they would have been initially recorded.

4.3. Considerations

It is to be noted that height estimates could not be completed for distances #7–15 with the 480p and 240p cameras, as visibility within these cameras' frames was very low and the placement of the timestamp in the frames obstructed the view of the farthest distances (see Fig. 11). Therefore, the results for cameras #6 (480p) and #7 (240p) were influenced by fewer data points. That said, the limited evidence present does suggest that accuracy was decreasing at cameras #6 (480p) and #7 (240p), based on some of the upward error trends for these cameras in Fig. 8. The association of the maximum error with camera #7 and distance point #1 is consistent with these trends.

Variables that have the potential to affect height estimation were controlled for or eliminated. The 'suspects' were captured on video walking along the path immediately after being measured, to eliminate the interference of spinal compression and its change to stature over the course of the day. Volunteers removed their hats and hoods, and their heights were measured with their shoes on so that they were wearing the same footwear as when caught on camera. One factor that could not be controlled for was the natural standing posture of the 'suspects'. Heights were recorded by one researcher, and the estimates were performed in PhotoModeler by the other researcher without knowing the actual height measurements to eliminate bias. The scene was cleared of obstructions and it was ensured that there was no interference with the equipment during the data collection process. The same pathway of distance markers in view of all cameras was used for all trials (i.e. same positions used), to eliminate the possibility for error that could have occurred if replicating distance points via creating separate pathways in front of each camera.

5. Conclusions

The purpose of this research was to examine if camera resolution and suspect-camera distance affect the accuracy and precision of photogrammetric height measurements. Up until distances of 36.5 m and 480p resolution, the accuracy of height estimates was fairly consistent. The accuracy decreased at greater suspect-camera distances, specifically those that exceeded 36.5 m. Analysts should also consider that distances too close to the camera (i.e. 2.6 m or less) may impact the accuracy of height estimates if the camera angle is steep in relation to a suspect's position; if, for example, a suspect is close to a camera but the camera is positioned straighter ahead, distance may not have an effect on measurement accuracy at all. Height estimates begin to decrease in accuracy when performed on stills of camera footage with resolution settings less than 960H. The maximum recorded measurement error was 3.4 cm, at a resolution of 240p and a distance of 2.6 m. This maximum error falls within an error threshold of 5% of total adult body height (i.e. the estimation error measures less than the 5% value of a given adult's height measurement), which is deemed here acceptable [21]. The minimum recorded measurement error was 0.1 cm, a result for multiple resolution settings and distances. Between 50–60 height estimates were correct measurements of suspects' heights (i.e. 0 cm error). The most frequently recorded measurement error was 0.2 cm.

This study was performed under optimal conditions where multiple variables that can be encountered in the field were controlled for. That considered, the majority of measurement errors (75%) were below +/- 1.3 cm. This result, and the maximum result, can act as a guideline for analysts and investigators when performing and considering the reliability of suspect height analysis for supporting evidence. Future research should examine a greater number of variables and their effect on the accuracy and precision of height estimates, such as hairstyles and headwear, as well as how these variables may interact with each other to impact measurement-taking. As the data suggests that camera-to-head angle may affect accuracy and precision at particular distances, this variable requires further study.

Funding

This research was funded by the University of Toronto Mississauga's Forensic Science Department and by ai2-3D

Forensics. Helen Guryn (ai2-3D Forensics) participated in study design, data collection, interpretation of analyses, and manuscript proofing. Eugene Liscio (ai2-3D Forensics) participated in resource provision, data collection as a volunteer study subject, and manuscript proofing. The decision to submit this manuscript for publication was supported by the University of Toronto Mississauga and ai2-3D Forensics.

Author contributions (CRediT statement)

Angela Olver: Formal analysis, Investigation, Writing – Original Draft, Visualization

Helen Guryn: Conceptualization, Methodology, Investigation, Resources, Writing – Review & Editing, Supervision, Funding acquisition

Eugene Liscio: Methodology, Resources, Writing – Review & Editing, Supervision, Funding acquisition

Contributors

Angela Olver has been involved in data collection, data analysis and preparation of the manuscript.

Helen Guryn has been involved in study design, data collection, data analysis and proofing of the manuscript.

Eugene Liscio has been involved in developing the PhotoModeler and laser scanner method, study design and proofing of the manuscript.

Declaration of Competing Interest

The authors declare that they have no known competing financial interests or personal relationships that could have appeared to influence the work reported in this paper.

Acknowledgements

The authors would like to thank Dr. Tracy Rogers of the Forensic Science program at the University of Toronto Mississauga, and the University of Toronto Mississauga for lending use of their campus parking facilities as the study area.

References

[1] D. DeAngelis, R. Sala, A. Cantatore, P. Poppa, M. Dufour, M. Grandi, et al., New method for height estimation of subjects represented in photograms taken from video surveillance systems, Int. J. Legal Med. 121 (2007) 489–492, doi:http://dx.doi.org/10.1007/s00414-007-0176-4.

[2] G. Edelman, I. Alberink, B. Hoogeboom, Comparison of the performance of two methods for height estimation, J. Forensic Sci. 55 (2) (2010) 358–365, doi:http://dx.doi.org/10.1111/j.1556-4029.2009.01296.x.

[3] C. BenAbdelkader, Y. Yacoob, Statistical body height estimation from a single image, Publication for the 8th IEEE International Conference on Automatic Face & Gesture Recognition (2008) 1–7, doi:http://dx.doi.org/10.1109/AFGR.2008.4813453.

[4] J.R. Williamson, Hazards of reverse projection from hand-held cameras, Proceedings in State-of-the-Art Mapping vol. 1943 (1993) 137–147, doi:http://dx.doi.org/10.1117/12.157140.

[5] P.K. Larsen, L. Hansen, E.B. Simonsen, N. Lynnerup, Variability of bodily measures of normally dressed people using PhotoModeler Pro 5, J. Forensic Sci. 53 (6) (2008) 1393–1399, doi:http://dx.doi.org/10.1111/j.1556-4029.2008.00874.x.

[6] P.K. Larsen, E.B. Simonsen, N. Lynnerup, Gait analysis in forensic medicine, J. Forensic Sci. 53 (5) (2008) 1149–1153, doi:http://dx.doi.org/10.1111/j.1556-4029.2008.00807.x.

[7] K.A. Meline, W.E. Bruehs, A comparison of reverse projection and laser scanning photogrammetry, J. Forensic Identif. 68 (2) (2018) 281–292.

[8] M. Johnson, E. Liscio, Suspect height estimation using the FARO Focus 3D laser scanner, J. Forensic Sci. 60 (6) (2015) 1–7, doi:http://dx.doi.org/10.1111/1556-4029.12829.

[9] M. Gasparovic, I. Malaric, Increase of readability and accuracy of 3D models using fusion of close range photogrammetry and laser scanning, Int. Arch. Photogramm. Remote Sens. Spatial Inf. Sci. 39 (B5) (2012) 93–98, doi:http://dx.doi.org/10.5194/isprsarchives-XXXIX-B5-93-2012.

[10] N. Lynnerup, M. Andersen, H.P. Lauritsen, Facial image identification using PhotoModeler, Leg. Med. 5 (3) (2003) 156–160, doi:http://dx.doi.org/10.1016/s1344-6223(03)00054-3.

[11] N. Ramstrand, S. Ramstrand, P. Brolund, K. Norell, P. Bergstrom, Relative effects of posture and activity on human height estimation from surveillance footage, Forensic Sci. Int. 212 (2011) 27–31, doi:http://dx.doi.org/10.1016/j.forsciint.2011.05.002.

[12] A.K. Chong, A rigorous technique for forensic measurement of surveillance video footage, Photogramm. Eng. Remote Sensing 68 (7) (2002) 753–759 doi:0099-1112/02/6807-753$3.00/0.

[13] I. Alberink, A. Bolck, Obtaining confidence intervals and likelihood ratios for body height estimations in images, Forensic Sci. Int. 177 (2008) 228–237, doi:http://dx.doi.org/10.1016/j.forsciint.2008.01.005.

[14] P. Russo, E. Gualdi-Russo, A. Pellegrinelli, J. Balboni, A. Furini, A new approach to obtain metric data from video surveillance: preliminary evaluation of a low-cost stereo-photogrammetric system, Forensic Sci. Int. 271 (2017) 59–67, doi:http://dx.doi.org/10.1016/j.forsciint.2016.12.023.

[15] S.O. Ismaila, O.E. Charles-Owaba, Determination of the highest permissible spinal shrinkage, Aust. J. Basic Appl. Sci. 2 (4) (2008) 872–875.

[16] J. Al-Baghdadi, H. Alizze, K. Abed Al-Hussein, Accuracy assessment of various resolutions digital cameras for close-range photogrammetry applications, J. Eng. 24 (9) (2018) 78–95, doi:http://dx.doi.org/10.31026/j.eng.2018.09.06.

[17] D. Dustin, E. Liscio, Accuracy and repeatability of the laser scanner and total station for crime and accident scene documentation, J. Assoc. Crime Scene Reconstr. 20 (2016) 57–67.

[18] H.W. Lilliefors, On the Kolmogorov-Smirnov test for normality with mean and variance unknown, J. Am. Stat. Assoc. 62 (318) (1967) 399–402.

[19] A.C. Elliott, L.S. Hynan, A SAS® macro implementation of a multiple comparison post hoc test for a Kruskal–Wallis analysis, Comput. Methods Programs Biomed. 102 (2011) 75–80, doi:http://dx.doi.org/10.1016/j.cmpb.2010.11.002.

[20] O.J. Dunn, Multiple contrasts using rank sums, Technometrics 6 (3) (1964) 241–252.

[21] P. Viswanath, I.A. Kakadiaris, S.K. Shah, A simplified error model for height estimation using a single camera, Publication for the 12th IEEE International Conference on Computer Vision Workshops (2009) 1259–1266, doi:http://dx.doi.org/10.1109/ICCVW.2009.5457466.